First presented at the 17th Q.M.W. Antenna Symposium, London, April 1991

THE GENTLEMAN'S GUIDE TO FREQUENCY SELECTIVE SURFACES

E.A. Parker

Electronic Engineering Laboratories

University of Kent

Canterbury, Kent, CT2 7NT UK

1. Introduction

Frequency selective surfaces or dichroics as they are alternatively known can be regarded as filters of electromagnetic waves, mainly in frequency, though they do find application in the angular spectrum [1]. There are two frequency sensitive processes which are commonly exploited in the design of these surfaces. One is the interference of waves reflected from cascaded partially transmitting boundaries (broadly similar to the Fabry Perot interferometers well known in optics), and the other is the resonant interaction of waves with segments of conductor - normally periodic arrays of conducting elements or slots in conducting screens. The cascaded boundaries could simply be the interfaces between stacked dielectric sheets, where the number of boundaries, their spacings and the dielectric permittivities are the quantities influencing the transmission response. Double or multiple layers of the metallic grids described later in these notes or cascaded arrays of elements can be employed, or more often in practice a combination of dielectric interfaces and arrays of elements. Waveguide has a high pass transmission characteristic - each mode has a cut-off frequency below which it is evanescent. This property is exploited in dichroic structures made up from stacks of short lengths of guide. Typically, these structures consist of metallic plates drilled with periodic arrays of circular apertures [2]. Below the cut-off frequency of the dominant TE_{11} mode they are highly reflecting, while above it there is a usable transmission region.

Areas where FSS have been applied include frequency separation in quasi optical beam splitters [3,4] dual or multi-banding Cassegrain reflectors [eg. 5-7], the provision of windows in metallic radomes [8], and in reflectors, phase screens for beam steering [9], beamwidth equalisation, and in dual band arrays [10]. These notes concentrate on important basic properties of FSS and do not discuss the electrical performance of individual antenna systems. Crosspolar effects are important to applications in communications. This is addressed in references 2, 6, 7 and in 11-14 for example.

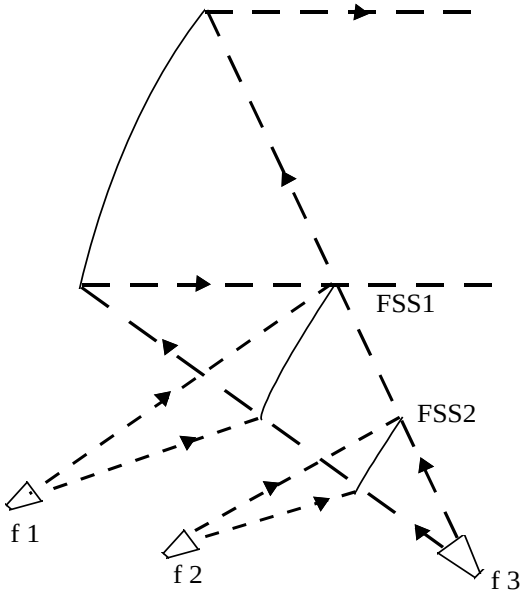

Fig.1: Three band offset reflector antenna

As an illustration of the application of FSS, Fig. I shows a scheme for providing 3 band operation of an offset reflector, using two cascaded dichroic subreflectors. The experimental performance of such a feed system has been described by Comtesse et al [17].

There are three principal techniques which are used for the analysis and design of FSS. The first is a modal analysis in which the distribution of current induced in conducting elements (or fields in slots) is represented as a series of suitable basis functions (usually sinusoidal functions or waveguide modes). Local fields are expanded as a set of Floquet modes [15] of the form

$$\psi_{pq} = \exp[- j\mathbf{k}_{pq} . \mathbf{r}] \exp[\pm j \gamma_{pq} z] \quad (1)$$

where r is a position vector in the x,y plane of the array, k_{pq} is a wave number determined by the lattice geometry and

$$\gamma_{pq} = \text{sqrt} (k^2 - \mathbf{k}_{pq}^2) \quad (2)$$

The two sets are matched by applying standard electromagnetic boundary conditions at the conductors. A resulting integral equation involving the element currents can be solved by the application of the method of moments [16,17] which generates a matrix equation for the coefficients of the current basis functions. This is a vector analysis and is capable of giving information about the polarisation of the scattered fields.

The second method is an equivalent circuit approach which models the arrays as lumped impedances on a transmission line [18]. Quasi empirical equivalent circuits have been

given [19] as design tools for quite complicated elements, requiring very little computing power. We shall return to this topic later.

The third technique is an Iterative process [20]. A first estimate of the element current induced by the incident field E_{inc} is used to calculate the local electric field distribution E, which is then forced to zero at the surface of the conductors. This modified field is in turn used to recalculate the element current distribution. The rms value of E/E_{inc} over the conductors can be used as an indicator of the progress of the iteration.

The first two of these techniques assume that the arrays are periodic and infinite in extent. The third is not restricted in these ways and variants [21] have been used to study edge effects and element currents across non uniformly illuminated FSS of finite size [22]. An interesting review of analysis techniques has been given by Mitra et al [23].

In the following sections, some of the more detailed properties of frequency selective surfaces and some of their limitations are illustrated.

2. Strip gratings and equivalent circuits

2.1 Strip gratings

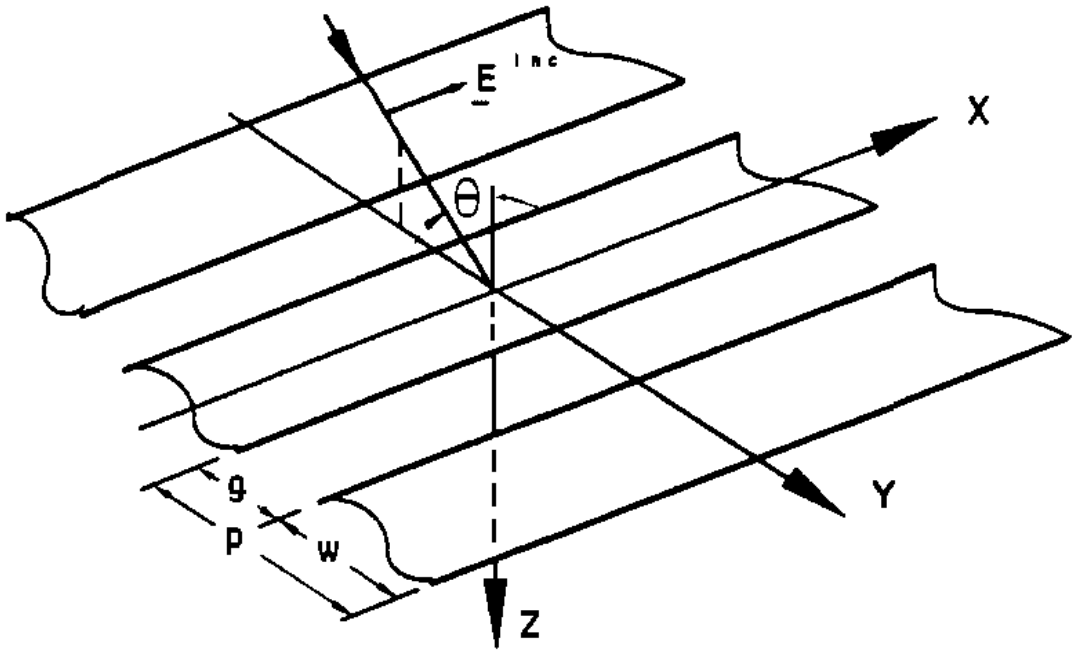

Fig. 2

Transmission through periodic arrays of conducting strips (Fig. 2) is frequency dependent and also depends on the orientation of the incident electric field relative to the strips. It can be modelled by using the analogy with a transmission line of characteristic impedance equal to that of free space, on which is mounted a lumped reactance representing the strip array [24]. When the tangential component of the incident electric field is parallel to the conductors (Fig. 2) this reactance is inductive, allowing very little transmission at low frequencies where the inductance virtually short circuits the line. The inductance decreases if the periodicity p decreases, or their width w increases and in consequence the transmission declines further, as would be expected as the grid approximates more closely

a solid metallic surface. The value of the inductance depends not only on p and w but also on the angle of incidence θ and on whether the incidence is TE or TM. The (normalised) reactances are

$$X_{TE,TM} = (p/\lambda)\cos\theta \cdot [\ln \operatorname{cosec}(\pi w/2p) + G_{TE,TM}(p, w, \lambda, \theta)] \quad (2)$$

$$= F(p, w, \lambda, \theta) \quad (2a)$$

where G is a correction term which is small compared with the ln cosec term. The capacitive susceptance (E field perpendicular to the strips) is

$$B_{TE,TM} = 4(p/\lambda)\cos\theta \cdot [\ln \operatorname{cosec}(\pi g/2p) + G_{TE,TM}(p, g, \lambda, \theta)] \quad (3)$$

$$= 4F(p, g, \lambda, \theta) \quad (3a)$$

check that when B is TE, TM G is also TE, TM and not TM, TE

These equations are valid at frequencies below the onset of the first grating lobe. So periodic arrays of long conducting strips or grids (periodic in x and y) have potential as frequency selective surfaces but they have the disadvantage that the transition from reflection to transmission occurs very slowly with frequency - typically at rates less than 6dB per octave. This can be remedied by cascading two or more layers of strips to take advantage of the multiple reflections between them.

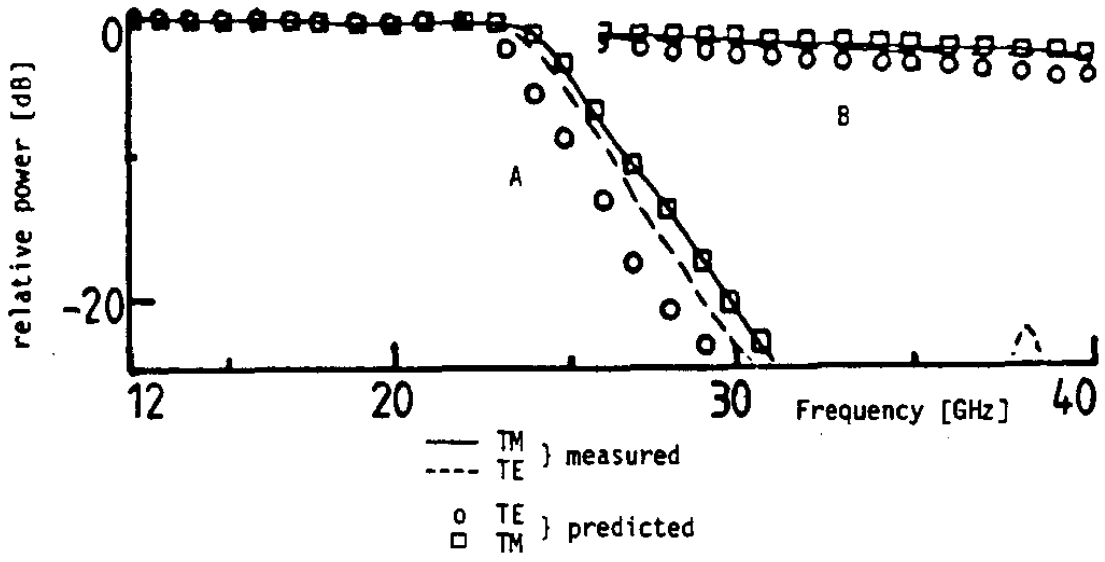

Fig.3: Measured and predicted plane wave transmission responses of capacitive patches at 45° incidence

A: 4 layers B: 1 layer

As an illustration, Fig. 3 shows the transmission response of 4 layers of capacitive patches measured in the frequency range 12-40 GHz. The transition between transmission and reflection occurs in the range 23-27 GHz, the ratio of the frequencies giving -10 dB and -0.5 dB transmission losses being slightly less than 1.2. The contrast with the slow fall of the superimposed curve for a single layer is clear. The four layers are separated by 3.2 mm, giving a structure which is almost a centimetre in depth. Depth is required with these non resonant arrays to give sufficient differential path length amongst the multiply reflected signals to sharpen the transmission responses. It is interesting to compare the transition rates provided by these multilayer structures with those typically available from waveguide plates of the same thickness.

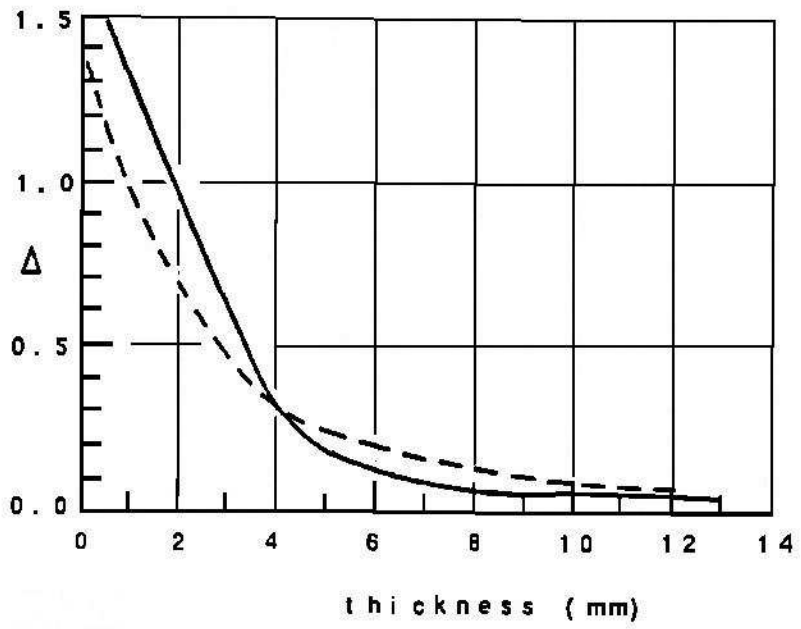

Fig.4

Fig. 4 plots the quantity |Δ| against the thickness t, where

$$\Delta = (f_{0.5} - f_{10}) / f_T \qquad (4)$$

and $f_{0.5}$, f_{10} and f_T are the -0.5 dB, -10dB and mid frequencies respectively in the transmission curves.

The two curves are similar.

2.2 Equivalent circuit models

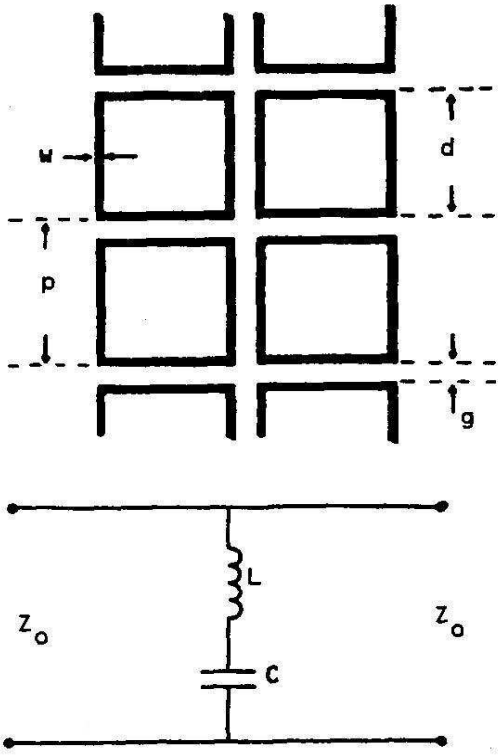

Fig.5: Array of square loops and equivalent circuit

Equivalent circuits are available for two complicated elements, the Jerusalem cross [18] and double square [19]. Fig. 5 shows the series LC equivalent circuit modelling the resonance of the simple square loop [25]. To compensate for the finite length d of the element segments and the gaps between them, the susceptance (eqn. 3a) at normal incidence is now

$$B = 4\,(d / \varepsilon_r\, p) \cdot F(p, g, \lambda) \qquad (5)$$

The reactance is

$$X = (d / p) \cdot F(p, 2w, \lambda) \qquad (6)$$

where the effective width is 2w, twice that of the conductors. The transmission coefficient of the array is then

$$T = 2jz / (1+2jz) \qquad (7)$$

where $z = X + B$. Table I shows the close agreement between the calculated and measured resonant frequencies of six arrays printed on a supporting dielectric substrate about 0.02 mm thick. The effective value of the relative permittivity ε_r in eqn. (5) was 1.1.

Table I: Experimental and calculated results for arrays of square loops

Array	Dimensions mm				Resonant frequency (normal wave incidence) GHz	
	p	w	d	g	Experimental	LC model
1	5.25	0.47	5.0	0.25	15.2	15.2
2	4.15	0.30	3.95	0.20	18.0	17.9
3	4.31	0.31	3.95	0.36	20.0	19.8
4	4.35	0.18	4.06	0.29	16.0	16.3
5	4.80	0.23	4.41	0.39	16.0	16.2
6	4.35	0.30	4.07	0.28	18.2	18.0

3. Resonant structures as array elements: dipoles

3.1 Linear dipoles

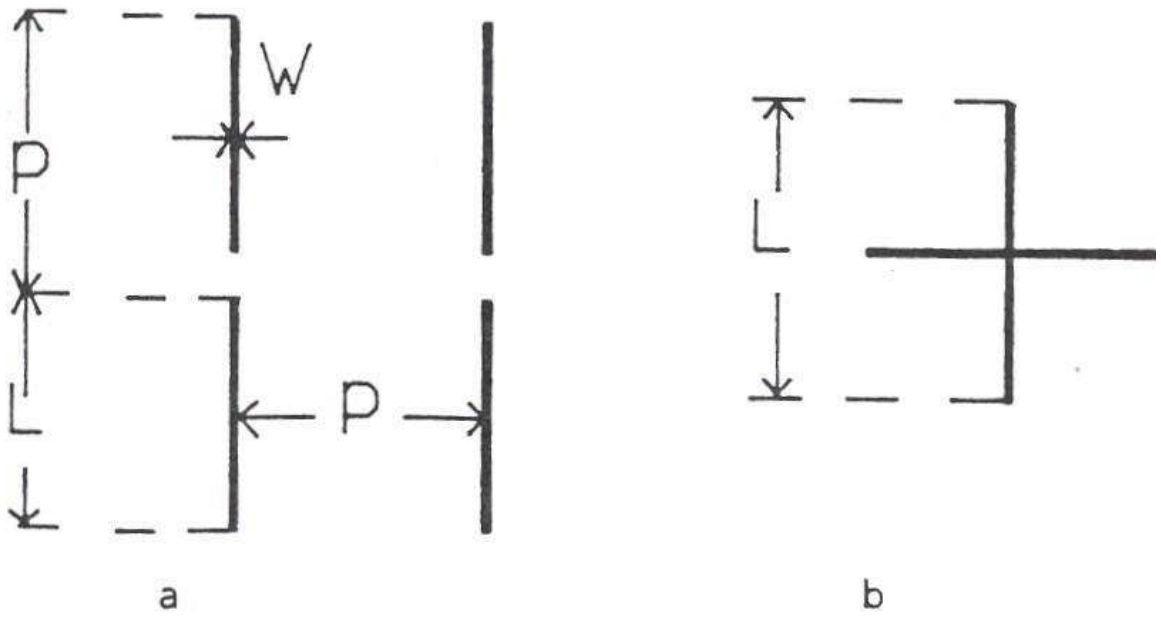

Fig.6: Linear and crossed dipoles

Arrays of linear dipoles (Fig. 6a) are amongst the simplest of configurations that have been used as frequency selective surfaces. Breaking up the infinitely long inductive strips forces currents induced by incident fields to zero at the ends of the segments. Although an equivalent circuit has been quoted [26] for these elements and is capable of giving an estimate of the transmission response, it is unable to describe the influence of one of the few variables associated with such simple arrays - the lattice geometry. It is a model which regards a dipole of length L as an open ended section of transmission line of length L/2, giving an impedance for a free standing array with a square lattice of periodicity p of

$$X = -1.7j \left(p^2 / L^2 \right) \cdot \eta_0 \cot(\pi L / \lambda.) \qquad (8)$$

which is in turn regarded as a lumped element across a line with free space characteristic impedance, as before. On the empirical basis used to construct LC equivalent circuits of more complicated elements, it is difficult to recognise capacitive components accurately. Dipole arrays are therefore often analysed using the modal technique. This requires more computer resources but once adopted gives a description of a greater range of array properties, including the current distribution within the elements and the state of polarization of the scattered fields. Linear dipoles offer the advantage over more complicated elements of requiring a minimal number of basis functions to synthesize the induced currents. Their relative simplicity has enabled factors such as the influence of supporting substrates or the effects of the finite sizes [27] of arrays in practice to be studied without making excessive demands on computer time.

One obvious limitation is their singly polarized structure. This can be overcome in the case of patch elements [5] by using crossed dipoles (Fig. 6b), at the expense of introducing more complicated current modes and their consequent modification of the transmission response (section 3.2, and reference 28). These modes represent current flows between the two orthogonal arms of the cross and can be attenuated by uncoupling the arms - for example by printing them on opposite sides of a thin dielectric substrate. This expediency is not available though in the case of their Babinet complements - arrays of slots in conducting sheets. Another factor, which can be a disadvantage when the required operating frequency bands are spread over a wide range of the surface transmission characteristic, is the relatively large lattice unit cell size in relation to their resonant wavelength [29], resulting in a small separation between the main reflection resonance and the frequency at which grating responses occur. We return to this question later.

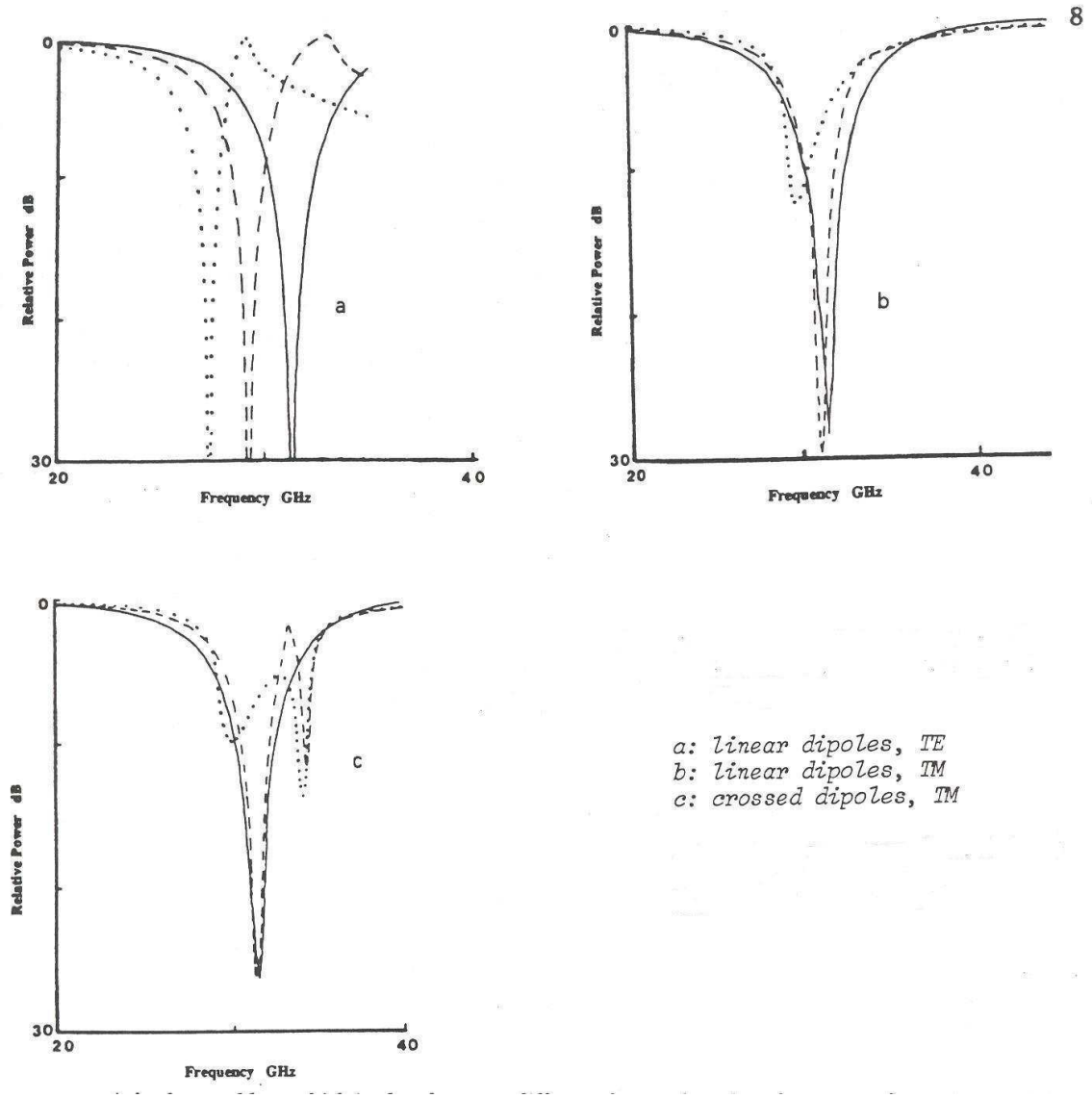

Fig.7: Transmission response of linear and crossed dipole arrays

a: linear dipoles, TE b: linear dipoles, TM c: crossed dipoles, TM

Solid curves: normal incidence

broken curves: 30°

curves with dots: 450

A further problem which is also shown to different degrees by other element configurations, and is typical of frequency selective surfaces generally, is their instability - the dependence of the transmission/frequency curves on the state of incidence of electromagnetic waves. Fig. 7 illustrates this effect well. It shows the transmission response of an array of linear dipoles with length L = 4.2 mm, arranged on the square lattice of side p = 6.0 mm sketched in Fig. 6a. The ratio L/p = 0.7. They are printed on a supporting substrate of thickness 0.8 mm with $\varepsilon_r = 2.3$. At normal incidence (with the E field parallel to the dipole axis) there is a reflection null at f_r just above 31 GHz, where the elements are approximately $\lambda/2$ in length. At low frequencies the surface is transparent.

The -0.5 dB band edge occurs at $f_t \sim 20$ GHz, giving a band separation ratio $f_r/f_t = 1.6$. As the angle of incidence increases, Fig. 7a shows that for TE incidence the resonance drifts downwards in frequency, to about 27 GHz at 45°. At the same time, the ratio f_r/f_t increases. The consequence can be serious for practical applications of such an array: there is no frequency band common to the three curves at the -10 dB level, which would represent the - 0.5 dB edges of the reflection band. The incidence would probably vary over this range across the surface of a Cassegrain subreflector. At 31 GHz, parts of the surface would reflect while others nearer the edges would not. This angle dependence is turned into an advantage and put to use in angle filters. Mailloux and colleagues [1] have used them to improve the sidelobe levels of antennas, attenuating signals at high angles.

In contrast, there is comparatively little drift in TM (Fig. 7b). The major effect is a narrowing of the reflection band. A characteristic property of conducting resonant elements is the narrowing of this band in TM and a broadening in it. The latter is masked in Fig. 7a by the proximity of the onset of grating responses. There, at normal incidence they occur at 50 GHz, but at 45° they appear at 29 GHz, (i.e. in the region of the reflection band), producing the initial sharp peak (related to a Wood's anomaly [15] near this frequency, but at higher frequencies removing energy from the main response. The shallowness of the TM 45^0 curve in Fig. 7b has a similar origin.

3.2 Crossed dipoles

The crossed dipole (Fig. 6b) is a more symmetrical element and offers the possibility of dual polarized operation. When arranged on the same lattice as before, their transmission response at normal and TE incidence is the same as that for linear dipoles, in Fig. 7a. But in TM the response is modified. A second null appears just above the main reflection resonance, near 35 GHz in Fig. 7c. Although the tangential component of the incident electric field is still parallel to the original dipole, at this additional resonance current now flows in the second arm of the element. The structure is excited in the asymmetrical mode sketched in Fig. 8.

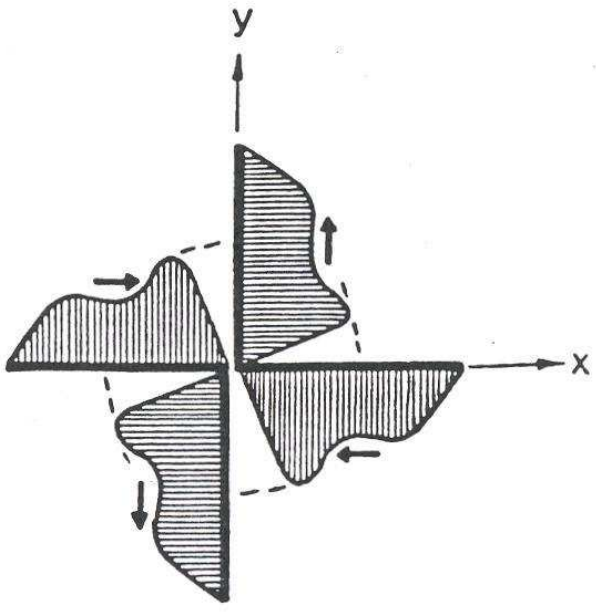

Fig.8: Asymmetrical resonance of a crossed dipole at oblique incidence.

This feature illustrates a general tendency: the more complicated the element configuration, the more complicated the transmission response curve. Once again this has its advantages and disadvantages. It can be used to modify the band ratios available from a surface, as in the case of the double square element [19]. On the other hand, subsidiary responses are undesirable if the intention is to design a surface with a single passband, as might occur in radome applications.

The influence of the array lattice geometry on the stability of the transmission response has been discussed for crossed dipoles in reference 28, and for the 3-legged element called a tripole in reference [30].

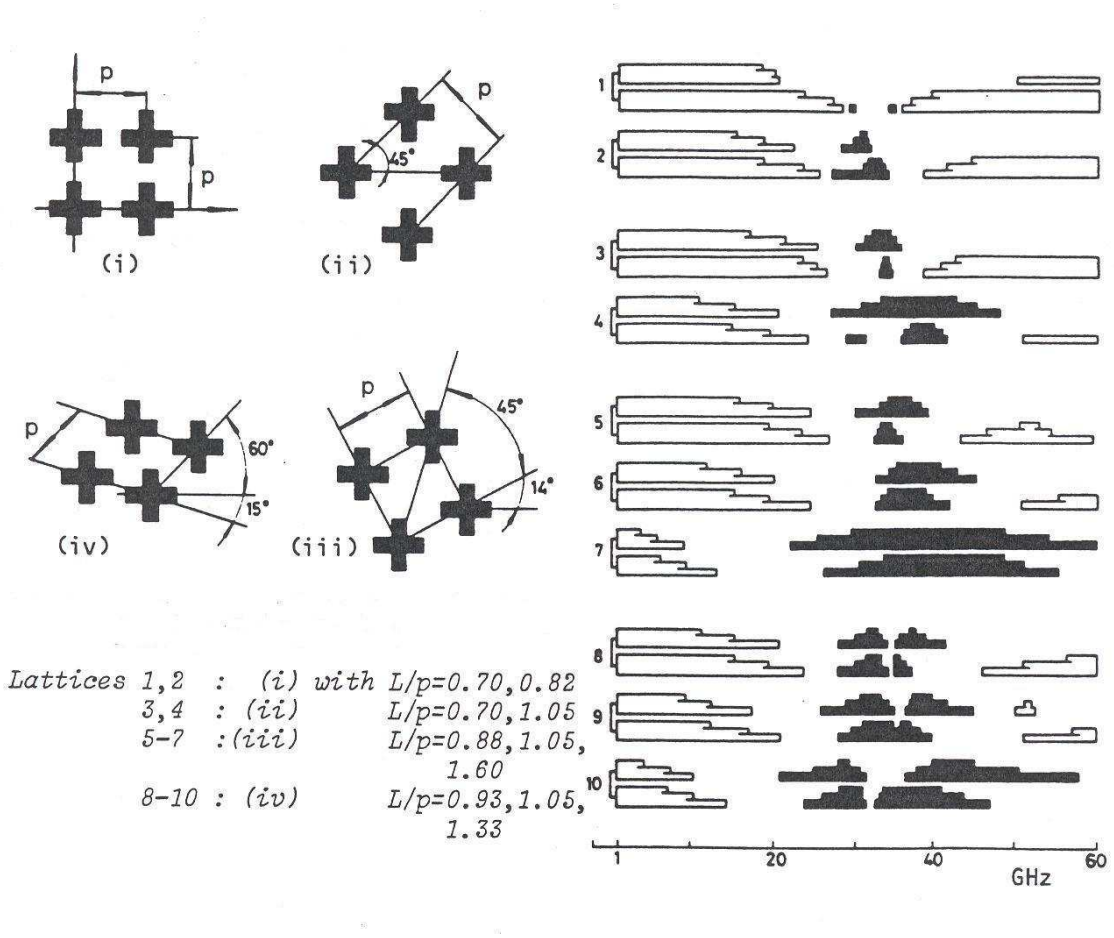

Fig.9: Crossed dipoles: transmission and reflection bands.

Fig. 9 shows the transmission and reflection bands to the -0.5, -1.0 and -2.0 dB points for crossed dipoles with L = 4.2 mm, printed on a thin substrate (0.75 mm thick, $\varepsilon_r = 2.3$) and set on the lattices illustrated. The linear dipoles in section 3.2 were on lattice 1.

There is a tendency for the more tightly packed arrays to have wider reflection bands and larger band separation ratios f_r/f_t . The split or double reflection band can be seen in some of these cases, and the improved performance of lattice 3 or the slightly rotated lattices 5 and 6 is clear. Johansson in reference 6 describes the design of an offset dichroic subreflector using a lattice similar to no.5, while Agrawal and Imbriale [5] designed a subreflector separating 2 and 14 GHz using lattice 4.

3.3 Convoluted dipoles

The instability of the reflection frequency f_r to angle of wave incidence θ is partly related to its proximity to the grating frequency

$$f_g = c/p(1 + \sin \theta) \qquad (9)$$

in which c is the velocity of the waves. In the modal analysis of the array the fields are expanded as a set of Floquet modes, all but one of which are evanescent below f_g. In the terms of a transmission line model the incident wave sees a reactance representing the array elements. Coupled to this line are higher order components corresponding to the other Floquet modes, the lowest of which begins to be significant as f_g is approached. In fact the admittance of the lowest TM mode becomes infinite at f_g .

Reducing the resonant frequency while retaining the unit cell size and periodicity p (or retaining the resonant frequency while reducing the unit cell size) raises the prospect of five advances:

(i) an improvement in the stability of f_r to angle of incidence;

(ii) the introduction of a usable transmission band above the reflection band;

(iii) increased separation of f_r from complicated features in the transmission curve above f_g

- potentially useful in the Babinet dual, where a transmission window would be further separated from other transmission regions above f_g;

(iv) easier drawing and less distortion of array elements on tightly curved surfaces - a topic which is not addressed in these notes.

(v) physically smaller unit cells – an advantage at long wavelengths.

One way in which this can be approached is to pack more resonant conductor length (and reactance generally) into the unit cell, i.e. by constructing a more complicated element (not forgetting the earlier remarks about the consequent possibility of further complicating the transmission curves).

An example is the modified dipole shown in Fig. 10, which has four cycles of convolution.

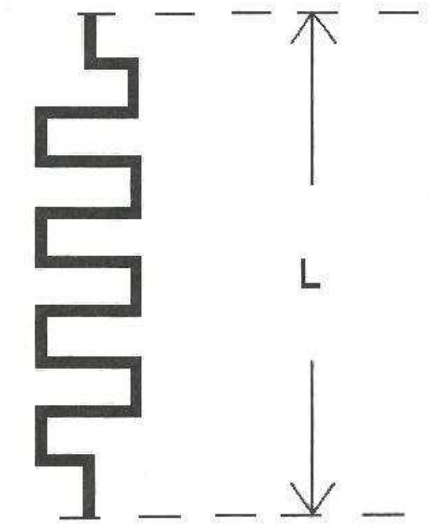

Fig.10: Convoluted dipole.

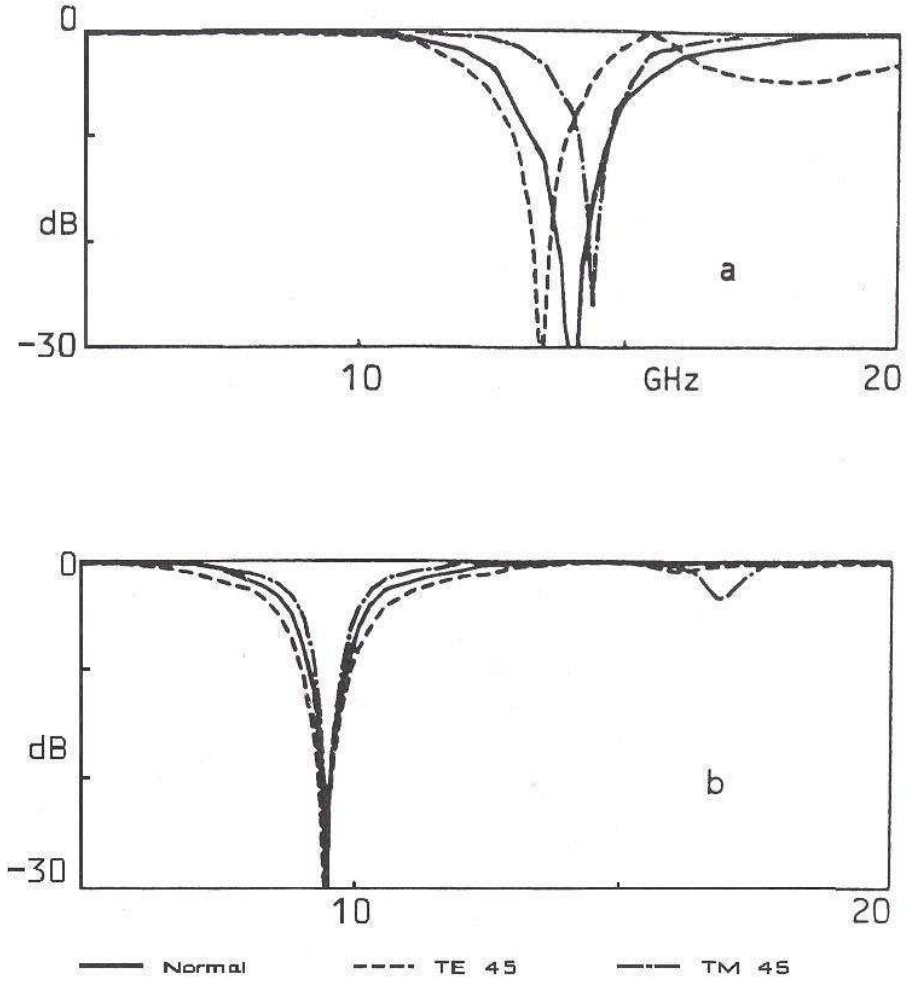

Fig.11: Measured transmission responses.

a: linear dipoles b: convoluted dipoles

Fig. 11 compares its measured transmission response with that of a standard linear dipole when both are set on a square lattice of periodicity p = 11.2 mm and printed on a substrate about 0.02 mm thick with $\varepsilon_r = 3$. They are both 9.5 mm long (L) but the total length of conductor in the convoluted dipole is 23 mm. The reflection frequency f_r has fallen from 14 GHz to 9.5 GHz, while the grating frequency f_g remains at 16 GHz at 45° incidence. The angular stability has clearly improved. In TM the reflection band still narrows as the angle of incidence increases but the much smaller drift of f_r in TE (about I percent) results in a 0.5 GHz bandwidth common to both states of incidence up to 45° at the -10 dB points. In an early study Munk [31] noted an improvement in stability with dipole slots loaded with an inductive loop. Note: this term 'convoluted' was coined and first used here and in reference 29 below.

3.4 Influence of supporting dielectric layers

For mechanical strength the array elements normally have to be placed on or in a suitable supporting dielectric structure, although of course slots in a conducting sheet can provide a free standing waveguide FSS. Even then, loading the slots with dielectric has the

advantage of lowering the cut-off frequency, increasing its separation from the onset of grating responses. The presence of the dielectric can have a major effect on the transmission response of the array. Aspects have been described by several authors, including Luebbers and Munk [32], Munk and Kornbau [33] and more recently in reference 34. Inserting conductors into dielectric layers has been regarded as a means of tuning out reflections from radome walls [35]. Appropriate choice of the dielectric structure can help to reduce the angular instability of the resonance frequency and bandwidth.

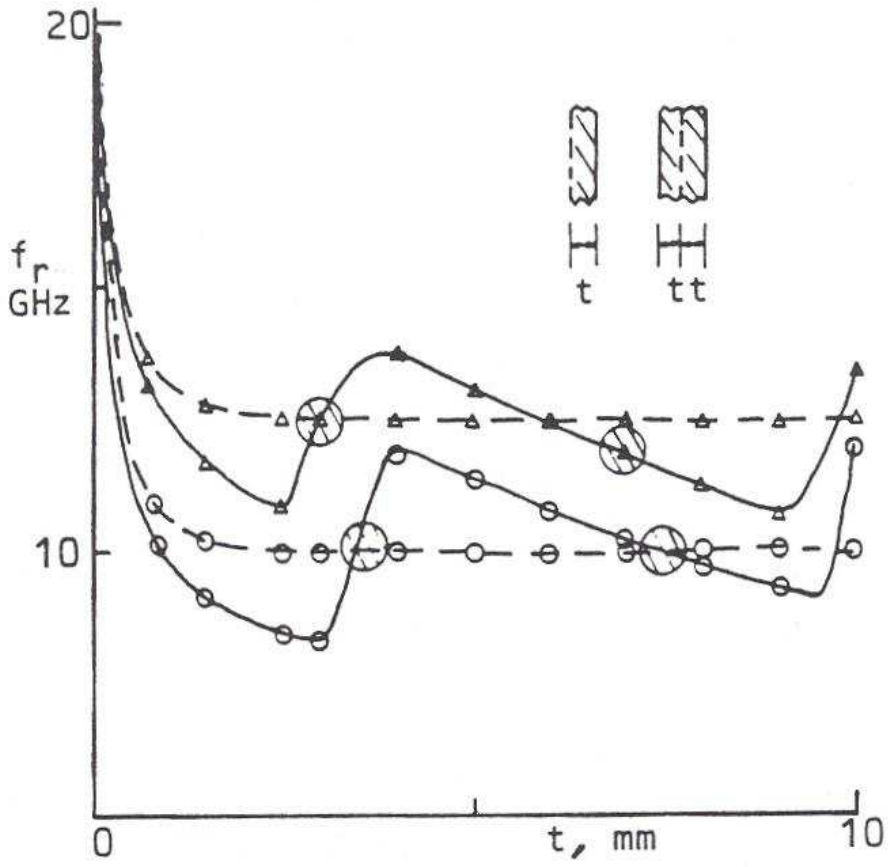

Fig.12: Variation of resonance frequency with dielectric thickness (normal incidence)
Continuous curves: dipole slots

broken curves: dipole patches

Δ: on o : in dielectric

Immersion of an array of conducting elements in an infinite dielectric of relative permittivity ε_r reduces the resonance and grating frequencies by a factor of $\sqrt{\varepsilon_r}$ so their ratio is unchanged. But mounting the elements on or in a dielectric layer of finite thickness introduces effects caused by the interaction of the fields adjacent to the conductors with the surfaces of the slab. Trapped waves can be set up. The most noticeable effect is the reduction of the resonance frequency and Fig. 12 shows its variation at normal incidence

for two arrays of dipoles and dipole slots as the thickness parameter t is increased, from 0 to 10 mm. They are set on lattice c of Fig. 9a, with L/p = 1.0. Here, $\varepsilon_r = 4$. For elements on the substrate, t is the total thickness and the related curves are shown by the triangles. Initially, as the thickness increases f_r declines rapidly in all four cases from the free space value of 20 GHz. In this range, low order evanescent Floquet modes decaying exponentially with distance from the elements still have significant amplitudes at the dielectric boundary.

The broken curve with circles shows that in the case of the conducting dipoles embedded in the layer, f_r approaches a limiting value of 10 GHz - i.e. $f_r^{air}/\sqrt{\varepsilon_r}$ as expected. The passband frequency of the slots (solid curve) also tends to this value but oscillates about the 10 GHz level. Near t = 4 mm and 10 mm (total thicknesses 8 and 20 mm) the overall passbands are wide and are the consequence of passbands generated by the dielectric itself sweeping through the passband of the slots. The difference between the two curves emphasises the fact that once the dielectric is present, the arrays are no longer Babinet complements. When the elements are mounted on the substrate the resonant frequency tends to a higher limiting value as the thickness increases, roughly equivalent to that when in an infinite medium with t equal to the mean of those of the two semi-infinite media. Consequently it is closer to the frequency where grating effects begin to occur.

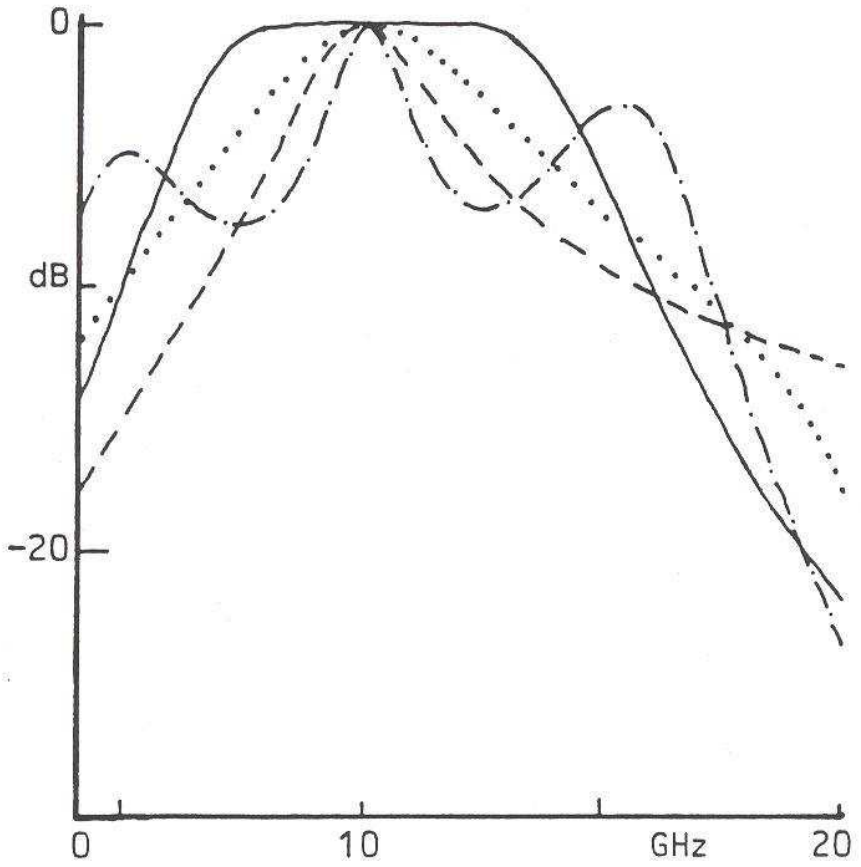

Fig.13: Transmission response of dipole slots in a dielectric layer of thickness 2t. $\varepsilon_r = 4$.
.... $2t = \infty$; - - - 2t = 2mm; — 2t = 7.5mm ; - . - . - . - 2t = 15mm.

Modification of the profile of the reflection or transmission band is an important effect of the dielectric slab. Fig. 13 illustrates the tuning of the slot array passband when inserted symmetrically in layers 2 mm, 7.5 mm and 15 mm thick. (The resonance frequency is relatively stable to angle of incidence for these values). The curve for the array in an infinite medium of $\varepsilon_r = 4$ is also included. As Fig. 12 suggests, f_r is close to 10 GHz in all these cases. With the 2 mm thickness, the -10 dB bandwidth is less than for the infinite case, while a thickness of one half wavelength at f_r (solid curve) gives a broad passband with a rapid roll-off at the edges, the -10 dB points being close to those for the infinite medium. Half wave dielectric panels are of course well known as non-reflecting windows.

3.5 Band spacings

Finally, a few brief comments about the band spacings available from single layer arrays of these simple resonant elements. If f_t is defined as the -0.5 dB edge of the low frequency transmission region of patch arrays, then the band spacing ratio f_r/f_t is limited by the broadening of the reflection band at oblique incidence. Fig. 9b gives a minimum value of about 2 for thin substrates, and nearer 2.5 when the thickness reaches 0.1 mm. If the -0.1 dB edge is chosen, then this ratio increases to 3 or more. Similar ratios can be deduced from Fig. 13 for slots in dielectric layers, although working to the lower band edge of the passband for the half wave panel can reduce the ratio to below 1.3. In general, complex elements or multiple layers must be used if small values are required, as described in section 2.

4. References

1 FRANCHI, P.R., and MAILLOUX, R.J.: 'Theoretical and experimental study of metal grid angular filters for sidelobe suppression', IEEE Trans., 1983, **AP-31**, pp. 445-450

2 LANGSFORD, P.A., and PARKER, E.A.: 'Cross-polarization of electromagnetic waves transmitted through waveguide dichroic plates', IEE Proc. H, 1981,**128**, pp. 1-5

3 COX, G.G, RUSSELL, P.J., and TUCKER, N.: 'Millimetre wave research demonstrator: antenna and optics subsystem', Marconi Space Systems research report, September 1988.

4 SALEH, A.A.M., and SEMPLAK, R.A.: 'A quasi optical polarization independent diplexer for use in beam feed system of millimetre wave antennas', IEEE Trans., 1976, **AP-24**, pp. 780-785

5 AGRAWAL, V.D., and IMBRIALE, W,A,: 'Design of a dichroic Cassegrain subreflector', IEEE Trans., 1979, **AP-27**, pp. 466-473

6 JOHANSSON, F.S,: 'Analysis and design of double layer frequency selective surfaces', IEE Proc. H, 1985, **132**, pp. 319-325

7 COMTESSE, L.E., LANGLEY, R.J., PARKER, E.A., and VARDAXOGLOU, J.C.: 'Frequency selective surfaces in dual and triple band offset reflector antennas', Proc. 17th European Microwave Conference, Rome, 1987, pp. 208-213

8 PELTON, EL., and MUNK, B.A.: 'A streamlined metallic radome', IEEE Trans., 1974, **AP-22**, pp, 799-803

9 GRIFFITHS, H,D., VERNON, A.M., and MILNE, K.: 'Planar phase shifting structures for steerable DBS antennas', Proc. 6th International Conference on Antennas and Propagation (ICAP 89), 1989, pp. 45-49

10 JAMES, J.R., and ANDRASIC, G.: 'Superimposed dichroic microstrip antenna arrays', IEE Proc. H., 1988, **135**, pp. 305-312

11 DERNERYD, A G., INGVARSON, P., JOHANSSON, F.S., PETTERSSON, L.E., and SHULEY, N.V.: 'Dichroic subreflector for satellite communications antenna applications', Proc. International Conference on Electromagnetics in Aerospace Applications, Turin, 1989, pp. 347-350

12 EL-MORSY, M.A.A., and PARKER, E.A.: 'A linearly polarized dual band diplexer in an offset reflector', J. lnstn. Electron. & Radio Engrs., 1986, **56**, pp. 111-116

13 BRESCIANI, D., and CONTU, S.: 'Comparison of dichroic structures for satellite applications', CSELT Technical Reports, 1985, **8**, pp. 91-96

14 MOK, T.S., ALLAM, A.M.M.A., VARDAXOGLOU, J.C., and PARKER, E.A.: 'Curved and plane frequency selective surfaces: a study of two offset subreflectors', J. Instn. Electron. & Radio Engrs., 1988, **58**, pp. 284-290

I5 AMITAY, N., GALINDO, V., and WU, C.P.: 'Theory and analysis of phased array antennas', (John Wiley & Sons Inc., 1972)

16 CHEN, C.C.: 'Scattering by a two dimensional periodic array of conducting plates', IEEE Trans., 1970, **AP-18**, pp. 660-665

17 MONTGOMERY, J.P.: 'Scattering by an infinite periodic array of thin conductors on a dielectric sheet', IEEE Trans., 1975, **AP-23**, pp. 70-75

18 ANDERSON, I.: 'On the theory of self resonant grids', Bell Syst. Techn. J., 1975, **54**, pp. 1725-1731

19 LANGLEY, R.J., and PARKER, E.A.: 'Double square frequency selective surfaces and their equivalent circuit', Electron. Lett., 1983, **19**, pp. 675-677

20 TSAO, C.C., and MITRA. R.: 'A spectral iteration approach for analysing scattering from frequency selective surfaces', IEEE Trans., 1982, **AP-30**, pp. 303-308

21 VAN DEN BERG, P.M.: 'Iterative computational techniques in scattering based upon the integrated square error criterion', IEEE Trans., 1984, **AP-32**, pp. 1063-1071

22 MOKHTAR, M.M., and PARKER, E.A.: 'Iterative computation of currents in frequency selective surfaces of finite size', Electron. Lett., 1989, **25**, pp. 221-222

23 MITTRA, R., CHAN, C.H., and CWIK, T.: 'Techniques for analysing frequency selective surfaces - a review', Proc. IEEE, 1988, **76**, pp. 1593-1615

24 MARCUWITZ, N.: 'Waveguide handbook (McGraw Hill, 1951)

25 LANGLEY. R.J., and PARKER, E.A.: 'Equivalent circuit model for arrays of square loops', Electron. Lett., 1982, **18**, pp. 294-296

26 ANDERSON, I.: 'Equivalent circuits for resonant grids', IEE colloquium on multiband techniques for reflector antennas', Digest No. 76, 1983

27 ALLAM, A.M.M.A., and PARKER, E.A.: 'Application of Pocklington's equation to analysis of dipole frequency selective surfaces of finite size', IEE Proc. H, 1987, **134**, pp. 521-526

28 HAMDY, S.M.A., and PARKER, E.A.: 'Influence of lattice geometry on transmission of electromagnetic waves through arrays of crossed dipoles', IEE Proc. H, 1982, **129**, pp. 7-10

29 PARKER, E.A., and EL-SHEIKH, A.N.A.: 'Convoluted array elements and reduced size unit cells for frequency selective surfaces', IEE Proc. H, 1991, **138**, pp.19-22

30 AU, P.W.B., MUSA, L.S., PARKER, E.A., and LANGLEY, R.J.: 'Parametric study of tripole and tripole loop arrays as frequency selective surfaces', IEE Proc. H, 1990, **137**, pp. 263-268

31 MUNK, B.A., KOUYOUMJIAN, R.G., and PETERS, L.: 'Reflection properties of periodic surfaces of loaded dipoles', IEEE Trans., 1971, **AP-19**, pp. 612-617

32 LUEBBERS, R.J., and MUNK, B.A.: 'Some effects of dielectric loading on periodic slot arrays', IEEE Trans., 1978, **AP-26**, pp. 536-542

33 MUNK, B.A., and KORNBAU, T.W.: 'On stabilization of the bandwidth of a dichroic surface by use of dielectric slabs', Electromagnetics, 1985, **5**, pp. 349-373

34 CALLAGHAN, P., PARKER, E.A., and LANGLEY, R.J.: 'Influence of supporting dielectric layers on the transmission properties of frequency selective surfaces', IEE Proc. H, 1991, **138**, pp. 448-454

35 GALLAGHER, J.G., and BRAMMER, D.J.: 'Scattering from an infinite array of periodic broken wires buried in a dielectric sheet', Radio Science, 1985, **20**, pp. 50-62